ACS APPLIED MATERIALS & INTERFACES

RESEARCH ARTICLE

www.acsami.org

A New Route to Size and Population Control of Silver Clusters on Colloidal TiO_2 Nanocrystals

Cao-Thang Dinh,[†] Thanh-Dinh Nguyen,[†] Freddy Kleitz,[‡] and Trong-On Do*[,†]

[†]Department of Chemical Engineering, Centre de recherche sur les propriétés des interfaces et la catalyse (CERPIC), [‡]Department of Chemistry and Centre de Recherche sur les Matériaux Avancés (CERMA), Laval University, Quebec G1 V 0A6, Canada

Supporting Information

ABSTRACT: Formation of hybrid Ag−TiO_2 nanocrystals (NCs) in which Ag clusters are uniformly deposited on individual TiO_2 NC surface has been achieved by using hydrophobic surfactant-capped TiO_2 NCs in combination with a photodeposition technique. The population of Ag clusters on the individual TiO_2 NC surface can be controlled by the degree of hydrophobicity (e.g., the number of vacant sites) on the TiO_2 NC surface while their size may be altered simply by varying irradiation time. A reversible change in color of the resulting hybrid Ag−TiO_2 NCs is induced by alternating UV light and visible-light illumination; however, the size and population of Ag clusters on TiO_2 NCs are almost unchanged. Furthermore, these materials also exhibit much higher photocatalytic performance as compared to that of Ag supported on commercial TiO_2−P25.

KEYWORDS: hybrid nanocrystals, Ag−TiO_2NCs, photodeposition, optical devices, photocatalysis

INTRODUCTION

Hybrid metal-semiconductor systems have been widely studied because of their unique catalytic and optoelectronic properties.[1−5] Among such systems, silver (Ag) nanoclusters supported on titania (TiO_2) have attracted substantial attention as they combine the advantages of a nontoxic, catalytically active metal showing size- and shape-dependent optical properties and a chemically stable, photoactive and low-cost semiconductor material.[6−10] In addition, interactions between Ag and TiO_2 at the nanoscale could result in new physical properties and enhanced catalytic activity.[7] Several approaches have been developed for the synthesis of Ag/TiO_2 hybrids including conventional impregnation, deposition−precipitation techniques, chemical reduction, photodeposition, and so on.[11−21] However, TiO_2 used in these approaches is usually under the form of an extended network rather than solution-stable TiO_2 NC species, thus Ag/TiO_2 hybrids with Ag deposited specifically on individual TiO_2 nanocrystals (NCs) are rarely obtained. Recently, Cozzoli et al.[22−25] have reported the synthesis of several hybrid materials based on TiO_2 NCs including organic-soluble Ag−TiO_2 composite using surfactant capped TiO_2 nanorods.[22] However, because of the large amount of surfactant covering the TiO_2 surface, no sites were available for Ag clusters to grow, and consequently, Ag particles grew in the solution instead of the TiO_2 NC surface. Although being challenging, the deposition of Ag clusters on individual TiO_2 NCs is highly desirable as it is expected to enhance the dispersion of active sites on TiO_2, and accordingly, their catalytic performance. Also, solution-stable hybrid metal-NCs are ideal for optical studies and represent important precursors for thin film processing.[26,27]

Herein, we report the synthesis of colloidal hybrid Ag−TiO_2 nanocrystals (namely Ag−TiO_2 NCs) in which Ag clusters are uniformly deposited on the surface of each individual TiO_2 NC. In addition to their high photocatalytic performance, these hybrid Ag−TiO_2 NCs also exhibit unique optical properties originated not only from the size-dependent surface plasmon resonance effect of silver clusters, but also from the synergistic interaction among Ag clusters and between Ag clusters and TiO_2 NCs. The central feature of our approach is the use of surfactant-capped TiO_2 NCs with different degrees of surface coverage as a nanosupport, in combination with a photodeposition technique. The starting TiO_2 NCs are well-dispersed in nonpolar solvent due to the hydrophobic surfactant-capped NC surface; however, they still possess a number of sites available on their surface for Ag growing. UV light irradiation of TiO_2 NC solution saturated with Ag ions leads to the reduction of Ag^+ adsorbed on uncapped TiO_2 surface sites by photogenerated electrons, and thus, to the formation of ultrasmall Ag clusters (Scheme 1). Moreover, by further addition of oleic acid (OA) in order to adjust the number of vacant sites on the TiO_2 NC surface, we are able to control the population of Ag clusters while their size may be altered simply by varying irradiation time.

EXPERIMENTAL SECTION

Chemicals. All chemicals were used as received; silver nitrate ($AgNO_3$), methylene blue (MB), titanium(IV) butoxide (TB, 97%), oleic acid (OA, 90%), and oleyl amine (OM, 70%) were purchased form Aldrich. Absolute ethanol and toluene solvents were of analytical grade and were also purchased from Aldrich.

Synthesis of TiO_2 Nanocrystals. The synthesis of TiO_2 nanocrystals was performed using the solvothermal method.[28] Typically, to synthesized TiO_2 nanorods with size of 15x50 nm, 20 mmol of TB was added to a mixture of 25 mmol OA, 25 mmol OM, and 100 mmol of absolute ethanol in a 40 mL Teflon cup. The resulting mixture was stirred for 10 min and subsequently transferred into a 100 ml Teflon-lined stainless steel autoclave containing 20 mL of a mixture of ethanol

Received: August 12, 2010
Accepted: June 15, 2011
Published: June 15, 2011

and water (96% ethanol, v/v). The system was then heated at 180 °C for 18 h. The obtained white precipitates were washed with ethanol and then redispersed in nonpolar solvent (toluene).

Synthesis of Colloidal Hybrid Ag−TiO_2 Nanocrystals. The as-synthesized TiO_2 nanocrystals were dispersed in toluene followed by the addition of different amounts of oleic acid (OA, in molar ratio relative to TiO_2) to vary surface coverage of TiO_2 NCs. $AgNO_3$ and ethanol were then added to the solution. The obtained mixture was de-aerated with a flow of nitrogen gas and exposed to UV light (365 nm) generated by a 100W Hg lamp at room temperature for different periods of time. For example, to synthesize hybrid Ag−TiO_2 NCs with a large amount of 2 nm Ag clusters, 5 mmol of as-synthesized TiO_2 nanocrystals were dispersed in 200 ml toluene with no additional OA. $AgNO_3$ (0.5g) and ethanol (2 mL) were then added to this solution. The solution was de-aerated by a flow of nitrogen gas for 30 minutes and then exposed to UV light for 1 minute. The resulting mixture was centrifugated to remove undissolved $AgNO_3$ before ethanol was added to precipitate hybrid Ag−TiO_2 NCs. The as-synthesized hybrid Ag−TiO_2 NCs powder was washed several times with ethanol in order to remove any remaining unreacted $AgNO_3$.

Scheme 1. Formation of Colloidal Hybrid Ag−TiO_2 NCs upon UV−Light Irradiation

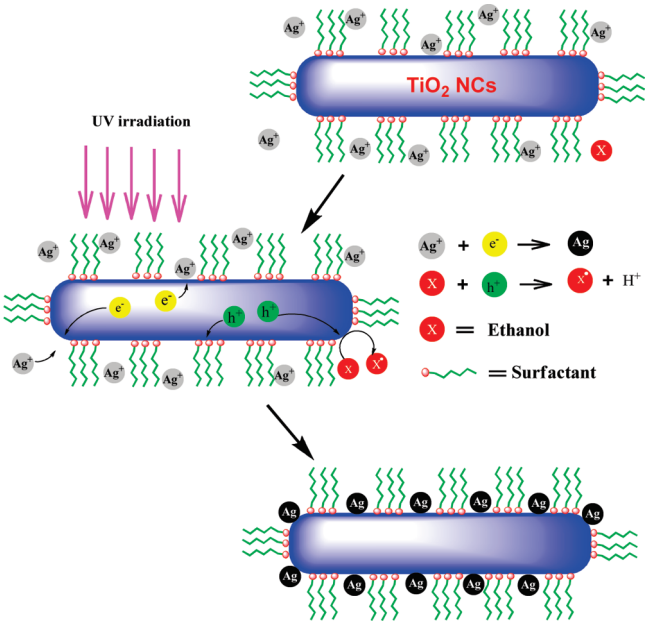

Characterization. Transmission electron microscopy (TEM) images of hybrid Ag−TiO_2 NCs were obtained on a JOEL JEM 1230 operated at 120 kV. Samples were prepared by placing a drop of a dilute toluene dispersion of nanocrystals onto a 200 mesh carbon-coated copper grid and evaporated immediately at ambient temperature. The Ag cluster size analysis was carried out by manually digitizing the high magnification TEM images with Image Tool. XPS measurements were carried out in an ion-pumped chamber (evacuated at 1×10^{-9} Torr) of a photoelectron spectrometer (Kratos Axis-Ultra) equipped with a focused X-ray source (Al K_α, $h\nu$ = 1486.6 eV). The binding energy of the samples was calibrated by setting the C 1 s peak to 285 eV. Peak deconvolution were performed by means of a standard CasaXPS software (v.2.3.13; product of CasaXPS Software Ltd., USA) to resolve the separate constituents after background substraction. Powder X-ray diffraction patterns of the samples were obtained on a Bruker SMART APEXII X-ray diffractometer equipped with a Cu K_α radiation source (λ = 1.5418 Å). Fourier transform infrared absorption spectra (FTIR) were measured with a FTS 45 infrared spectrophotometer with the KBr pellet technique. The UV-visible absorbance spectra were recorded on a Cary 300 Bio UV-visible spectrophotometer. The thermal analyses of the as-made hybrid Ag−TiO_2 NCs were carried out at a heating rate of 10 °C/min under a nitrogen flow up to 700 °C using a Perkin-Elmer TGA thermogravimetric analyzer. The silver loading content in hybrid Ag−TiO_2 NCs was determined by ICP-MS.

Photocatalysis. Before photocatalytic testing, the surfactants adsorbed on TiO_2 surface were removed. For the pure TiO_2 NCs, the

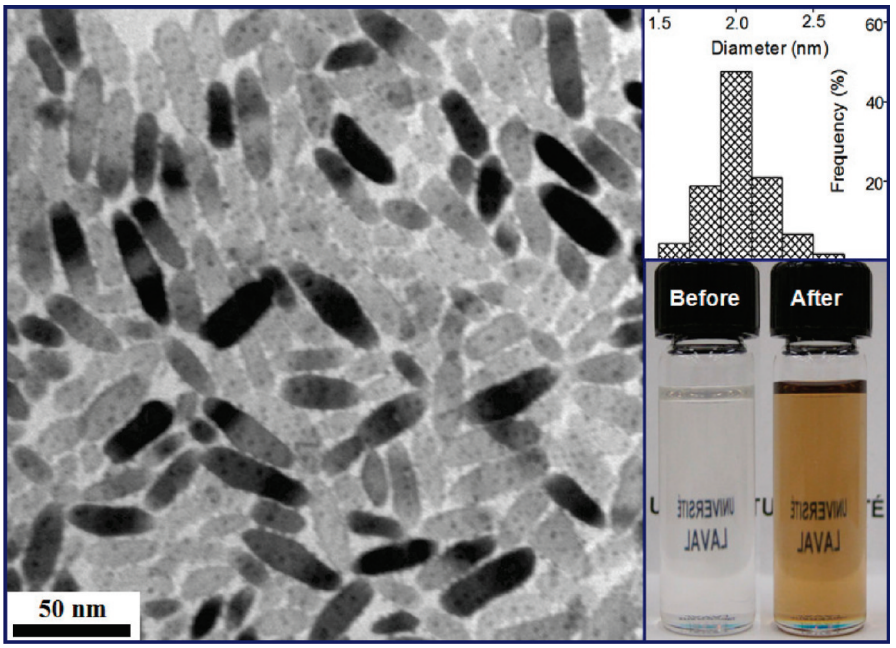

Figure 1. TEM image of hybrid Ag−TiO_2 NCs (2.6 % mol Ag) synthesized from a solution of TiO_2 nanorods containing silver nitrate without additional OA, after UV irradiation (1 minute). Insets are size distribution of Ag clusters (upper) and photograph of the Ag−TiO_2 NC solution before and after irradiation (lower).

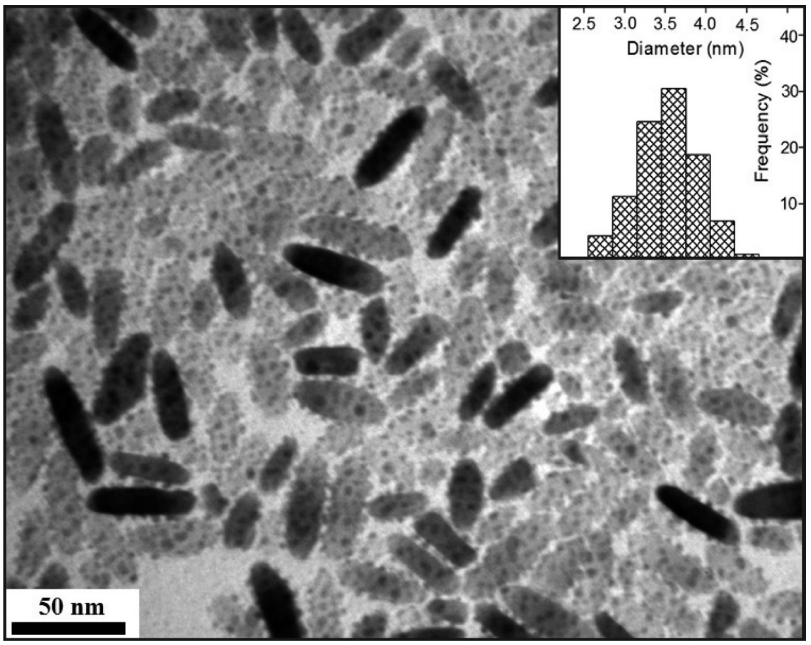

Figure 2. TEM image of hybrid Ag−TiO_2 NCs synthesized from a solution of TiO_2 nanorods containing silver nitrate without additional OA, after UV irradiation (40 min). Inset is size distribution of Ag clusters.

surfactants were removed as previously reported.[29] For hybrid Ag−TiO_2 NCs, the surfactants were removed by irradiating hybrid Ag−TiO_2 NCs dispersed in water for 3 h. The resulting mixture was then centrifugated to obtain a surfactant-free hybrid Ag−TiO_2 NCs powder. This powder was dried overnight at 60 ^{0}C and used as such for photocatalytic test. Photocatalytic activities of the samples were evaluated by the photocatalytic decomposition of Methylene Blue (MB). A mixture of MB aqueous solution (20 ppm, 30 ml) and the given photocatalyst (30 mg) was magnetically stirred in absence of light for 30 min to ensure adsorption-desorption equilibrium between the photocatalyst and MB. The mixture was then stirred under UV-vis irradiation using a 100 W Hg lamp. At given time intervals, 3 mL of the suspension was collected and centrifuged to remove photocatalyst particles. UV-vis absorption spectrum of the centrifugated solution was recorded using a Cary 300 Bio UV−visible spectrophotometer to determine the conversion of the reaction.

RESULTS AND DISCUSSION

Figure 1 and Figure S1 in the Supporting Information show transmission electron microscopy (TEM) images of the hybrid Ag−TiO_2 NCs synthesized by irradiating a mixture of TiO_2 nanorods, which were obtained by our recently developed method,[28] silver nitrate and ethanol in toluene for a period of 1 min. As clearly seen, a large number of Ag clusters with uniform size (ca. 2 nm) were highly dispersed on the TiO_2 NC surface. In addition, no separated Ag clusters or particles were observed implying that Ag clusters grew selectively on the individual TiO_2 NC surface. Importantly, the synthesis solution remained transparent upon irradiation, but the solution color changed from colorless to light brown, which is indicative of the formation of metallic Ag clusters (inset in Figure 1). The Ag content in the hybrid NCs was 2.6 (% mole) as obtained from ICP-MS analyses. The oxidation state of the Ag species was confirmed by X-ray photoelectron spectroscopy (XPS). As shown in Figure S2 in the Supporting Information, the Ag $3d_{5/2}$ peak at a binding energy of 368.0 eV is characteristic of metallic Ag.[30] The crystallinity of TiO_2 and size of Ag clusters were also confirmed by powder X-ray diffraction (XRD). The XRD patterns of the hybrid Ag−TiO_2 NCs (see Figure S3 in the Supporting Information) exhibit well-defined and intense peaks that are assigned to the pure anatase phase with high crystallinity. However, no XRD peaks of Ag were detected, indicating very small size of Ag clusters.

It is well-known that band-gap illumination of TiO_2 creates electron-hole pairs which move to the surface and are consumed for reduction and oxidation reactions.[31] In our system, the surface electrons both act as reducing agents for the conversion of Ag+ ions to metallic Ag and as negative charges for attracting Ag+ ions to the TiO_2 surface, whereas the holes are consumed for the oxidation of ethanol or surfactants present in the system. Once the metallic Ag atoms are created, Ag clusters can be formed located on the TiO_2 surface either by aggregation of concurrently formed Ag atoms (eq 1), or by a sequence of alternating electronic and ionic events similar to the photographic process (eq 2).[32]

$$mAg^0 \rightarrow Ag_m \quad (1)$$

$$Ag^0 + Ag^+ \rightarrow (Ag)_2^+ \xrightarrow{+e^-} Ag_2 + Ag^+$$
$$\rightarrow (Ag)_3^+ \xrightarrow{+e^-} Ag_3 \rightarrow \ldots \rightarrow Ag_m \quad (2)$$

However, the presence of surfactants adsorbed on the TiO_2 NC surface is expected to hinder both the migration of Ag atoms on the TiO_2 surface as well as Ag^+ ions from approaching the TiO_2 surface. Thus, this phenomenon will slow down the growth of Ag clusters on TiO_2 surface, resulting in very small Ag clusters. Consequently, the slow growth of Ag clusters enables us not only to fabricate hybrid Ag−TiO_2 NCs with uniform and very small size of Ag clusters, but also to control the size of these clusters simply by varying irradiation time. We have thus performed experiments with longer irradiation time (40 min) and it was found that the size of Ag clusters increased from 2 nm to about 3.5 nm with no noticeable change in the number of clusters as

well as the initial TiO_2 NC morphology (Figure 2 and S4). However, along with the increase in cluster size, the solution stability of the hybrid NCs is decreasing as the irradiation time is prolonged. In fact, a precipitation of Ag−TiO_2 NCs was found to occur with extending irradiation time to 60 minutes (see Figure S5 in the Supporting Information). Most likely, this could originate from two reasons. The first one is the photooxidation of the surfactant molecules present on the TiO_2 NC surface, which ultimately decreases the overall hydrophobic character of the hybrid NCs. To clarify this point, we have performed thermogravimetric analysis (TGA) of the two hybrid Ag−TiO_2 NCs samples obtained after 40 and 60 min of irradiation. The results (see Figure S6 in the Supporting Information) revealed that the weight loss in the temperature range of 150−450 °C, which belongs to the decomposition of surfactant molecules,[33,34] is 2.7 and 2.0%, respectively, for these two samples. This indicates that a fraction of the surfactants has been removed upon extending irradiation time. It is noted that in the presence of Ag clusters on the surface, the photogenerated electrons in TiO_2 NCs are trapped by the metal clusters, therefore the photo-holes can exhibit a longer lifetime, leading to enhanced photooxidation properties.[31,35] In addition, photo-holes in our system can be scavenged by ethanol or OA molecules adsorbed on the TiO_2 surface. Nevertheless, when the vacant sites are occupied by metal clusters, the accessibility of ethanol molecules to the TiO_2 surface is dramatically reduced. Thus, the photo-holes should mainly be scavenged by OA, resulting in a progressive oxidation of these molecules on the TiO_2 NC surface. The second reason that may cause the precipitation of hybrid Ag−TiO_2 NCs is an increase of the surface fraction occupied by the Ag domains which are not protected by surfactant along with longer irradiation time. To identify this, we have used oleylamine surfactant, which is known to be easily adsorbed on the surface of metal particles[36,37] in order to protect the surface of metallic Ag clusters. Accordingly, a small amount of oleylamine was added to the hybrid Ag−TiO_2 NC solution after 40 min of irradiation. Interestingly, the hybrid NCs were stable in solution for more than 60 minutes of additional irradiation. This result indicates that the surface of Ag nanoparticles indeed plays an important role in the solution stability of the hybrid Ag−TiO_2 NCs. However, in the presence of oleylamine, together with the increase in Ag cluster size as the irradiation time was prolonged, we observed the formation of some isolated Ag nanoparticles (which were detached from TiO_2 NC surface) (see Figure S7 in the Supporting Information).

It should be noted that the formation of hybrid Ag−TiO_2 NCs using our approach is quite different from that of metal−TiO_2 nanocomposites reported in refs 22 and 23. The TiO_2 NCs used in our approach exhibit a number of vacant sites for the formation of very small Ag clusters on the TiO_2 NC surface. Because of their high surface free energy due to the small size, these clusters are strongly adhering to the TiO_2 NCs surface. In contrast, in the above references, a large amount of surfactant molecules remained adsorbed on the TiO_2 nanorod surface, leading to Ag growing only on high surface energy points such as tips of the TiO_2 nanorods, which resulted ultimately in Ag nanoparticles that are stabilized by TiO_2 nanorods through electrostatic interactions.[22] To verify the presence of vacant sites on the surface of TiO_2 NCs, we have performed O1s XPS analysis of as-synthesized TiO_2 NCs as illustrated in Figure S8 in the Supporting Information. The peak at 529.9 eV can be ascribed to the oxygen in the lattice of TiO_2 NCs, while the peak at 531.3 eV is attributed to the oxygen of surface hydroxyl (−OH) groups.[38−40] The last peak located at 532.2 eV binding energy can be explained by the presence of surface carboxylic (COO−) groups.[40,41] The presence of hydroxyl and carboxylic groups on the surface of TiO_2 NCs was also evidenced by the FTIR spectrum of as-made TiO_2 NCs, as seen in Figure S9 in the Supporting Information. Two bands at 1454 and 1551 cm^{-1} are attributed to the symmetric and asymmetric stretching vibrations of the carboxylate groups;[29,34] a large band around 3400 cm^{-1} corresponds to the O−H stretching frequency of hydroxyl groups on the surface of TiO_2 NCs.[29,34] This result suggests that, both hydroxyl and carboxylic groups are presented on the surface of TiO_2 NCs. As the hydroxyl groups are believed to act as the sites for the growth of Ag clusters, hybrid Ag−TiO_2 NCs with a large number of Ag clusters on TiO_2 surface can thus be easily obtained. It is worth mentioning that, the surface properties of TiO_2 NCs is depending on the synthesis procedure. In our study, TiO_2 NCs were produced by hydrolytic condensation of both carboxylalkoxide and hydroxyalkoxide.[28] The hydrolytic condensation of hydroxyalkoxide yields a large amount of hydroxyl groups on the TiO_2 NC surface. These results thus confirm that the amount of surfactants adsorbed on the TiO_2 NC surface plays a key role in the formation of hybrid Ag−TiO_2 NCs. On the other hand, it is known that carboxylic acids readily adsorb on the TiO_2 surface.[42,43] We have thus added OA to the TiO_2 NC solution before the addition of $AgNO_3$ in order to decrease the amount of vacant sites on the NC surface with the objective of varying the number of formed Ag clusters. Using an OA:TiO_2 molar ratio of 1:1 and after 40 min of irradiation, only a few Ag clusters with the size of 5−10 nm were deposited on the TiO_2 NC surface (Figure 3A). The XRD pattern of this sample, as shown in Figure S10 in the Supporting Information, exhibits diffraction peaks attributed to the anatase phase and signals corresponding to the silver nanocrytals. The particle size of silver nanoparticles as calculated using the Scherrer equation was about 7.3 nm, in good agreement with the TEM results. It should be mentioned that the solution remains saturated with Ag ions during irradiation as an excess amount of $AgNO_3$ was used. A small number of formed Ag clusters can be explained by the presence of large amounts of OA adsorbed on TiO_2, which considerably limit the adsorption of Ag ions on the TiO_2 surface. When the amount of additional OA was reduced ten times (i.e., OA:TiO_2 molar ratio of 0.1:1), a larger number of Ag clusters with a size about 5 nm were formed on the TiO_2 NC surface after 40 min of UV irradiation (Figure 3B). These results demonstrate that, in our case, the surfactant-capped TiO_2 NCs act not only as nanoreactors for the formation

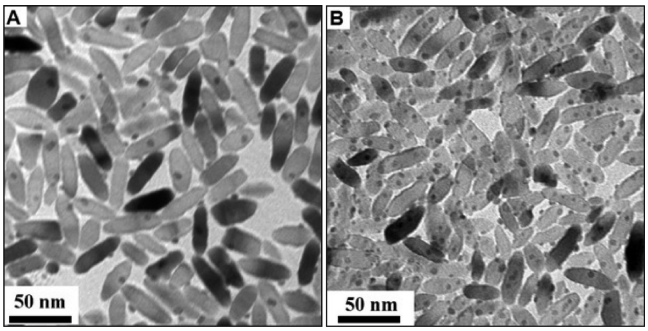

Figure 3. TEM images of the hybrid Ag−TiO_2 NCs synthesized by additional OA and irradiated for 40 min. (A) OA:TiO_2 = 1:1, and (B) OA:TiO_2 = 0.1:1.

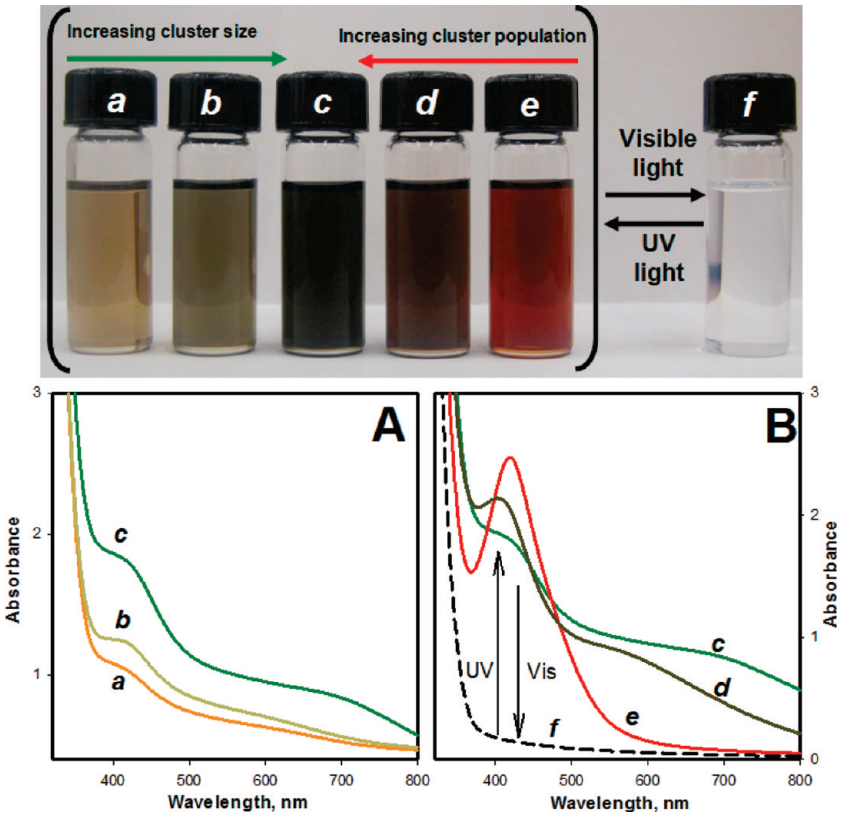

Figure 4. UV−vis absorption spectra of the hybrid Ag−TiO_2 NCs with different sizes (A) synthesized without additional OA and irradiated for (a) 1 min, (b), 10 min, and (c) 40 min, and different populations of Ag clusters, (B) synthesized with (e) OA:TiO_2 = 1:1, (d) OA:TiO_2 = 0.1:1, and (c) without OA (bottom panel), and photographs of the corresponding solutions (top panel). (f) UV−vis spectrum (bottom panel, B) and the photograph (top panel) of a hybrid Ag−TiO_2 NC solution after being exposed to visible light for 1 day.

of Ag clusters with different size, but also as substrates for the formation of desired populations of Ag clusters on their surface.

The optical properties of hybrid Ag−TiO_2 NCs exhibiting different Ag cluster sizes and populations were analyzed by UV−vis spectroscopy. As seen in Figure 4A, the UV−vis spectra of the hybrid Ag−TiO_2 NCs synthesized without an addition of OA at different irradiation times exhibit an absorption band at around 410 nm along with a pronounced tail towards higher wavelengths. These two resonances may arise from the surface plasmon band of Ag clusters and an interparticle coupling effect influencing the surface plasmon resonance, respectively.[44−47] The relative weak absorption peak at around 410 nm can be associated to the small size of Ag clusters. By extending the irradiation time, the absorption band at about 410 nm was red-shifted, which can be attributed to the size-dependent surface plasmon resonance effect of metallic Ag;[48] size of Ag cluster increases with increasing irradiation time, while the tail at about 700 nm grew in intensity and the color of the solution changed from light brown to dark green (vials a−c). The UV−vis spectra of the hybrid Ag−TiO_2 NCs with different Ag cluster populations are depicted in Figure 4B. As clearly seen in Figure 4B, the UV−vis spectrum of the hybrid Ag−TiO_2 NCs with a few Ag clusters (corresponding to the TEM image in Figure 3A) exhibits a strong absorption peak at 420 nm (curve − in Figure 4B). However, no tailed resonance at higher wavelength was observed indicating no interparticle coupling effect. In fact, this spectrum of the hybrid material is rather similar to that of colloidal Ag nanoparticles.[49,50] By increasing the population of Ag clusters, the interparticle coupling effect became more noticeable as the resonance at higher wavelength is being red-shifted and growing in intensity (curves c and d in Figure 4B, corresponding to the TEM images in Figure 2 and Figure 3B, respectively). Also, the color of the solution changed from red to brown and to dark green as the population of Ag clusters increases (vials e, d, and c).

Along with the optical properties arising from the Ag clusters, hybrid Ag−TiO_2 NCs also exhibit photochromic properties due to the interaction between Ag clusters and TiO_2 NCs. To identify that, the hybrid Ag−TiO_2 NC solutions with different sizes and populations of Ag clusters were exposed to visible light (day light) for one day in the presence of air. The colorless solution (Figure 4, vial f, top panel,) was observed for all the samples after visible light illumination. A representative UV−vis spectrum of these colourless solutions is shown in Figure 4B (curve f). No absorption bands in the visible region were observed. The disappearance of the absorption bands in this region could be explained by the oxidation of Ag clusters to Ag^+ ions by oxygen in air under visible light.[7,51] Interestingly, the initial colors of these solutions could be recovered by removing air and re-exposing the sample to UV light (365 nm). This indicates a reversible change in color induced by alternating UV light and visible light; however, the size and population of Ag clusters on TiO_2 NCs remained almost unchanged (see Figure S11 in the Supporting Information). We propose that, after being formed from the oxidation of metallic Ag, the Ag^+ ions may still be adsorbed on TiO_2 surface possibly at the same sites of metallic Ag

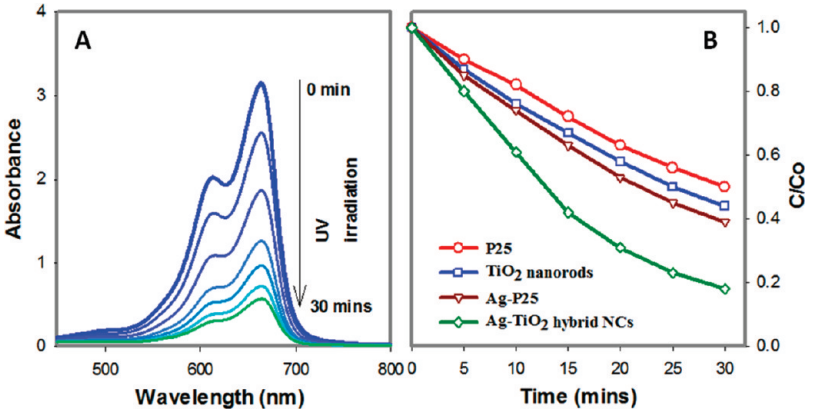

Figure 5. (A) UV−vis absorption spectra of a methylene blue (MB) solution as a function of irradiation time in the presence of hybrid Ag−TiO_2 NCs catalyst, and (B) comparison of the MB photodegradation using TiO_2 nanorods, P25, Ag−P25, and hybrid Ag−TiO_2 NCs as photocatalysts.

clusters. Therefore, when that solution was re-exposed to the UV light, the preformed Ag^+ ions were reduced back to Ag at the same location as that of the metallic Ag clusters resulting in almost similar hybrid Ag−TiO_2 NCs to those before being exposed to the visible light. Our results reveal that a fine control of the size and population of the Ag clusters on the TiO_2 NC surface could result in hybrid Ag−TiO_2 NCs exhibiting various optical properties ranging from those of colloidal Ag nanoparticles to those of their aggregates. Therefore, multicolor hybrid Ag−TiO_2 NCs, which have potential applications in a variety of fields,[7,52] can be obtained with their properties depending on size and population of Ag clusters on the TiO_2 NC surface.

To evaluate the photocatalytic performance of the thus-obtained hybrid Ag−TiO_2 NCs, we used NCs with Ag clusters of 2 nm and a 2.6 % mol Ag loading as an example (sample in Figure 1) in the photocatalytic decomposition of methylene blue (MB). For comparison, pure TiO_2 nanorods, commercial P25 and Ag−P25 composites synthesized using the same photodeposition technique with comparable Ag loading (2.8 % mole), were also used. Figure 5A shows the spectra of the MB solution as a function of time over the hybrid Ag−TiO_2 NCs catalyst. The absorption band at 660 nm, which is characteristic of MB, decreases in intensity with increasing irradiation time, this being an indication of the decomposition of MB. The results, as shown in Figure 5B, indicate that the pure TiO_2 nanorods exhibit a slightly higher catalytic activity than that of P25. This may be due to a shape effect on the photocatalytic efficiency.[29] Both hybrid Ag−TiO_2 materials show higher photocatalytic activity than that of pure TiO_2 materials. However, the hybrid Ag−TiO_2 NCs clearly exhibit a much higher performance for the photocatalytic degradation of MB as compared to Ag−P25. The high photocatalytic activity of Ag−TiO_2 NCs could be due to a very high dispersion of Ag clusters on the individual TiO_2 NCs.

Finally, our synthesis procedure has also been extended to other shapes of TiO_2 NCs. As illustrated in Figure S12 in the Supporting Information, hybrid Ag−TiO_2 NCs with dog-bone and rhombic TiO_2 NC shapes were also successfully synthesized with and without additional OA. These results offer opportunities to investigate the influence of the TiO_2 NC shapes in the hybrid Ag−TiO_2 system on both photocatalytic and oxidative reactions. Attempts for the synthesis of hybrid Ag−TiO_2 NCs with a wider range of Ag cluster sizes are currently underway in our laboratory.

CONCLUSION

In summary, we have demonstrated a new synthesis of hybrid Ag−TiO_2 NCs using a facile photodeposition technique. Small Ag clusters are highly dispersed on individual TiO_2 NC surface. Our method can be used to control both the population of Ag clusters by tuning the amount of OA added in the synthesis solution, and their size by irradiation time. The thus-obtained hybrid Ag−TiO_2 NCs exhibit highly photocatalytic performance and unique optical properties ranging from those of colloidal Ag nanoparticles to those of aggregates of Ag nanoparticles. In addition, these hybrid NCs also exhibit a reversible change in their color which was induced by alternating UV light and visible light illumination. As perspectives, this approach may be extended to other metals, such Au, Pt, Pd, and other semiconductor supports for the synthesis of wide variety of new hybrid metal−semiconductor NC systems.

ASSOCIATED CONTENT

Supporting Information. Additional TEM images, XRD, XPS, FTIR, and TGA data of hybrid Ag−TiO_2 NCs. This material is available free of charge via the Internet at http://pubs.acs.org.

AUTHOR INFORMATION

Corresponding Author
*E-mail: trong-on.do@gch.ulaval.ca.

ACKNOWLEDGMENT

This work was supported by the Natural Sciences and Engineering Research Council of Canada (NSERC) through a strategic project. C.T.D. thanks the Fonds Québécois de la Recherche sur la Nature et les Technologies (FQRNT) for the merit scholarship.

REFERENCES

(1) Mokari, T.; Rothenberg, E.; Popov, I.; Costi, R.; Banin, U. *Science* **2004**, *304*, 1787–1790.
(2) Casavola, M.; Grillo, V.; Carlino, E.; Giannini, C.; Gozzo, F.; Pinel, E. F.; Garcia, M. A.; Manna, L.; Cingolani, R.; Cozzoli, P. D. *Nano Lett.* **2007**, *7*, 1386–1395.

(3) Subramanian, V.; Wolf, E. E.; Kamat, P. V. *J. Am. Chem. Soc.* **2004**, *126*, 4943–4950.
(4) Casavola, M.; Buonsanti, R.; Caputo, G.; Cozzoli, P. D. *Eur. J. Inorg. Chem.* **2008**, 837–854.
(5) Carbone, L.; Cozzoli, P. D. *Nano Today* **2010**, *5*, 449–493.
(6) Fujishima, A.; Honda, K. *Nature* **1972**, *238*, 37–38.
(7) Ohko, Y.; Tatsuma, T.; Fujii, T.; Naoi, K.; Niwa, C.; Kubota, Y.; Fujishima, A. *Nat. Mater.* **2003**, *2*, 29–31.
(8) Chen, X.; Mao, S. S. *Chem. Rev.* **2007**, *107*, 2891–2959.
(9) Zhang, H.; Wang, G.; Chen, D.; Lv, X.; Li, J. *Chem. Mater.* **2008**, *20*, 6543–6549.
(10) Sun, T.; Seff, K. *Chem. Rev.* **1994**, *94*, 857–870.
(11) Halasi, Gy.; Kecskeméti, A.; Solymosi, F. *Catal. Lett.* **2010**, *135*, 16–20.
(12) You, X.; Chen, F.; Zhang, J. J.; Anpo, M. *Catal. Lett.* **2005**, *102*, 247–250.
(13) Haneda, M.; Kintaichi, Y.; Inaba, M.; Hamada, H. *Catal. Today* **1998**, *42*, 127–135.
(14) Herrmann, J. M.; Disdier, J.; Pichat, P. *J. Catal.* **1988**, *113*, 72–81.
(15) Wu, T. S.; Wang, K. X.; Li, G. D.; Sun, S. Y.; Sun, J.; Chen, J. S. *ACS Appl. Mater. Interfaces* **2010**, *2*, 544–550.
(16) Wodka, D.; Bielanska, E.; Socha, R. P.; Wodka, M. E.; Gurgul, J.; Nowak, P.; Warszynski, P.; Kumakiri, I. *ACS Appl. Mater. Interfaces* **2010**, *2*, 1945–1955.
(17) Zhang, H.; Chen, G. *Environ. Sci. Technol.* **2009**, *43*, 2905–2910.
(18) Chen, S. F.; Li, J. P.; Qian, K.; Xu, W. P.; Lu, Y.; Huan, Q. X.; Yu, S. H. *Nano Res.* **2010**, *3*, 244–255.
(19) Zhang, H.; Li, X.; Chen, G. *J. Mater. Chem.* **2009**, *19*, 8223–8231.
(20) Zhang, F.; Pi, Y.; Cui, J.; Yang, Y.; Zhang, X.; Guan, N. *J. Phys. Chem. C* **2007**, *111*, 3756–3761.
(21) Chan, S. C.; Barteau, M. A. *Langmuir* **2005**, *21*, 5588–5595.
(22) Cozzoli, P. D.; Comparelli, R.; Fanizza, E.; Curri, M. L.; Agostiano, A.; Laub, D. *J. Am. Chem. Soc.* **2004**, *126*, 3868–3879.
(23) Cozzoli, P. D.; Curri, M. L.; Giannini, C.; Agostiano, A. *Small* **2006**, *2*, 413–421.
(24) Buonsanti, R.; Grillo, V.; Carlino, E.; Giannini, C.; Gozzo, F.; Hernandez, M. G.; Garcia, M. A.; Cingolani, R.; Cozzoli, P. D. *J. Am. Chem. Soc.* **2010**, *132*, 2437–2464.
(25) Buonsanti, R.; Grillo, V.; Carlino, E.; Giannini, C.; Curri, M. L.; Innocenti, C.; Sangregorio, C.; Achterhold, K.; Parak, F. G.; Agostiano, A.; Cozzoli, P. D. *J. Am. Chem. Soc.* **2006**, *128*, 16953–16970.
(26) Cozzoli, P. D.; Pellegrino, T.; Manna, L. *Chem. Soc. Rev.* **2006**, *35*, 1195–1208.
(27) Talapin, D. V.; Lee, J. S.; Kovalenko, M. V.; Shevchenko, E. V. *Chem. Rev.* **2010**, *110*, 389–458.
(28) Dinh, C. T.; Nguyen, T. D.; Kleitz, F.; Do, T. O. *ACS Nano* **2009**, *3*, 3737–3743.
(29) Joo, J.; Kwon, S. G.; Yu, T.; Cho, M.; Lee, J.; Yoon, J.; Hyeon, T. *J. Phys. Chem. B* **2005**, *109*, 15297–15302.
(30) Wagner, C. D.; Riggs, W. M.; Davis, L. E.; Moulder, J. F. *Handbook of X-Ray Photoelectron Spectroscopy*; Perkin-Elmer Corp., Physical Electronics Division: Eden Prairie, MN, 1979.
(31) Linsebigler, A. L.; Lu, G.; Yates, J.T., Jr. *Chem. Rev.* **1995**, *95*, 735–758.
(32) Disdier, J.; Herrmann, J. −M.; Pichat, P. *J. Chem. Soc., Faraday Trans.* **1983**, *79*, 651–660.
(33) Nguyen, T. D.; Dinh, C. T.; Do, T. O. *Langmuir* **2009**, *25*, 11142–11148.
(34) Nguyen, T. D.; Dinh, C. T.; Do, T. O. *ACS Nano* **2010**, *4*, 2263–2273.
(35) Hoffmann, M. R.; Martin, S. T.; Choi, W.; Bahnemann, D.W. *Chem. Rev.* **1995**, *95*, 69–96.
(36) Chen, M.; Feng, Y. G.; Wang, X.; Li, T. C.; Zhang, J. Y.; Qian, D. J. *Langmuir* **2007**, *23*, 5296–5304.
(37) Peng, S.; McMahon, J. M.; Schatz, G. C.; Gray, S. K.; Sun, Y. *Proc. Natl. Acad. Sci. U.S.A.* **2010**, *107*, 14530–14534.
(38) McCafferty, E.; Wightman, J. P. *Surf. Interface Anal.* **1998**, *26*, 549–564.
(39) Chen, X.; Liu, L.; Ya, P. Y.; Mao, S. S. *Science* **2011**, *331*, 746–750.
(40) Schmidt, M.; Stainemann, S. G. *Fresenius J. Anal. Chem.* **1991**, *341*, 412–415.
(41) Liu, C.; Yang, S. *ACS Nano* **2009**, *3*, 1025–1031.
(42) Kamat, P. V.; Barazzouk, S.; Hotchandani, S. *Angew. Chem., Int. Ed.* **2002**, *41*, 2764–2767.
(43) Robel, I. N.; Subramanian, V.; Kuno, M.; Kamat, P. V. *J. Am. Chem. Soc.* **2006**, *128*, 2385–2393.
(44) Storhoff, J. J.; Lararides, A. A.; Mucic, R. C.; Mirkin, C. A.; letsinger, R. L.; Shatz, G. C. *J. Am. Chem. Soc.* **2000**, *122*, 4640–4650.
(45) Ghosh, S. K.; Pal, T. *Chem. Rev.* **2007**, *107*, 4797–4862.
(46) Peng, S.; Lei, C.; Ren, Y.; Cook, R. E.; Sun, Y. *Angew. Chem., Int. Ed.* **2011**, *50*, 3158–3163.
(47) Kelly, K. L; Coronado, E.; Zhao, L. L.; Schatz, G. C. *J. Phys. Chem. B* **2003**, *107*, 668–677.
(48) Kleemann, W. Z. *Z. Phys.* **1968**, *215*, 113–120.
(49) Henglein, A. *J. Phys. Chem.* **1993**, *97*, 5457–5471.
(50) Wang, W.; Efrima, S.; Regev, O. *Langmuir* **1998**, *14*, 602–610.
(51) Naoi, K.; Ohko, Y.; Tatsuma, T. *J. Am. Chem. Soc.* **2004**, *126*, 3664–3668.
(52) Ditlea, S. *Sci. Am.* **2001**, *285*, 38–43.